A Case Study in Hexahedral Mesh Generation: Simulation of the Human Mandible

C. Kober*
Freie Universität Berlin

M. Müller–Hannemann**
Friedrich-Wilhelms-Universität Bonn

Abstract

We provide a case study for the generation of pure hexahedral meshes for the numerical simulation of physiological stress scenarios of the human mandible. Due to its complex and very detailed free-form geometry, the mandible model is very demanding.

This test case is used as a running example to demonstrate the applicability of a combinatorial approach for the generation of hexahedral meshes by means of successive dual cycle eliminations which has been proposed by the second author in previous work. We report on the progress and recent advances of the cycle elimination scheme. The given input data, a surface triangulation obtained from computed tomography data, requires a substantial mesh reduction and a suitable conversion into a quadrilateral surface mesh as a first step, for which we use mesh clustering and b-matching techniques.

Several strategies for improved cycle elimination orders are proposed. They lead to a significant reduction in the mesh size and a better structural quality. Based on the resulting combinatorial meshes, gradient-based optimized smoothing with the condition number of the Jacobian matrix as objective together with mesh untangling techniques yielded embeddings of a satisfactory quality.

To test our hexahedral meshes for the mandible model within an FEM simulation we used the scenario of a bite on a "hard nut." Our simulation results are in good agreement with observations from biomechanical experiments.

Keywords. Cycle elimination scheme, FEM simulation, hexahedral mesh generation, human mandible, quadrilateral mesh generation, optimized mesh smoothing

*Dr. Cornelia Kober, Freie Universität Berlin, Institut für Mathematik II, WE2, Arnimallee 2-6, 14195 Berlin, Germany, ckober@math.fu-berlin.de.

**Dr. Matthias Müller-Hannemann, Rheinische Friedrich-Wilhelms-Universität Bonn, Institut für Diskrete Mathematik, Lennéstr. 2, 53113 Bonn, Germany, muellerh@or.uni-bonn.de; www.math.tu-berlin.de/~mhannema.
Correspond with the second author.

1 Introduction and Background

In a wide range of applications of numerical simulations by means of the finite element method (FEM) the generation of hexahedral meshes is highly desirable. However, in spite of enormous research efforts, the robust generation of such meshes with an acceptable quality is still a challenge for complex domains.

Several promising approaches for hexahedral mesh generation work as follows: Given a prescribed quadrilateral surface mesh they first build the combinatorial dual of the hexahedral mesh. This dual mesh is converted into the primal hexahedral mesh, and finally embedded and smoothed into the given domain. Two such approaches, the modified Whisker Weaving algorithm by Folwell and Mitchell [1], as well as a method developed by the second author [2], rely on an iterative elimination of certain dual cycles in the surface mesh. An intuitive interpretation of the latter method is that cycle eliminations correspond to complete sheets of hexahedra in the volume mesh.

The purpose of this paper is twofold: on the one hand, we want to report recent progress with our combinatorial cycle elimination approach. On the other hand, we provide a case study of its application to the stress analysis of a human mandible model. The study comprises the full meshing process, starting from a given initial triangulation, the conversion to a quadrilateral surface mesh, the hexahedral mesh generation, and finally an illustrative test case for the analysis run on the created hexahedral mesh.

To get an impression of the input complexity, see Fig. 1 for the mandible model given as a triangulation with 35432 triangles.

1.1 Application background

Numerical simulations are widely used in the field of biomechanics for the prediction of regional stress and stress-compatibility. In particular, experts in the field of biomechanics and medical research are interested in a deeper understanding of the mechanical behavior of the

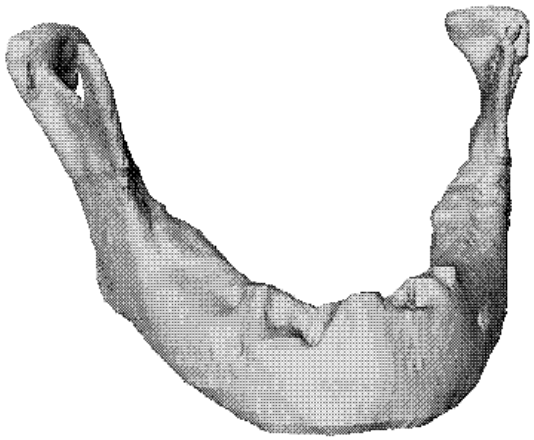

Figure 1: View on the given mandible model.

human mandible. Our part in a project with H.-F. Zeilhofer and R. Sader from the department of Oral and Maxillofacial Surgery at the University of Technology Munich lies in the mathematical modeling, the simulation, and as a prerequisite, the generation of a hexahedral mesh.

Current work points are the simulation of traumatologic standard situations [3] and the validation of the modeling by resimulation of standard movements like closing of the mouth, adduction and retraction [4]. The long term goal is the development of a software tool allowing individual numerical simulation of the human jawbone. To give a few examples, the idea is to apply such a tool in a clinical setting as a planning aid for difficult operations, the design of implants, the layout of prostheses for large bone deficiencies, and the optimization of new methods for osteosynthesis [5].

As a consequence, this implies for the mesh generation process that we need relatively coarse meshes to ensure that we can realize short computation times with a moderately sized hardware equipment. Our coarsest mesh for the mandible model consists of only 1300 quadrilaterals and 2252 hexahedra. This allows to run the FEM simulation on an ordinary workstation. Another justification for coarse meshes lies in the fact that we have to face several sources of imprecision in the whole experiment, for example, coming from assumptions about the modeling of the material or the load case. Hence, it makes no sense to ask for a very fine mesh which would prelude an accuracy which is already lost in other parts of the experiment.

On the other hand, an appropriate degree of the coarseness has to be determined. Thus, the computation with such extremely coarse meshes as we used requires a validation of the simulation results with finer meshes. As a first step in this direction, we refined our coarse mesh in such a way that the refined surface mesh is a submesh of the coarser one, simply by subdivision of each quadrilateral into four new ones. By that, we can specify comparable boundary conditions in the FEM simulation.

1.2 Hexahedral Mesh Generation

We briefly review methods for hexahedral mesh generation starting with a quadrilateral surface mesh. This restriction is justified by several reasons, most importantly by the fact that only such methods can guarantee mesh compatibility between subdomains, either naturally induced by different material or artificially created to simplify the mesh decomposition of the remaining parts.

For a more general overview, we refer to the recent survey articles of Schneiders [6] and Owen [7], for online information and data bases on meshing literature see [8] and [9].

We distinguish between a *combinatorial phase* in which a cell complex of hexahedra, a so-called *hex complex*, is constructed, and the *embedding phase* which yields the final hexahedral mesh. The theoretical basis for the combinatorial phase has been laid by Thurston [10] and Mitchell [11]. They characterized independently the combinatorial properties of quadrilateral surface meshes which can be extended to hexahedral meshes. Namely, for a domain which is topologically a ball and which is equipped with an all-quadrilateral surface mesh, there exists a combinatorial hexahedral mesh without further boundary subdivision if and only if the number of quadrilaterals is even. Furthermore, Eppstein [12] used this existence result and proved that a linear number of hexahedra (in the number of quadrilaterals) are sufficient in such cases. These results, however, are not fully constructive and they do not tell how to derive a geometric embedding of a combinatorial mesh with an acceptable quality.

Advancing front based methods like *plastering* [13, 14] maintain throughout the algorithm the *meshing front*, that is a set of quadrilateral faces which represent the boundary of the region(s) yet to be meshed. These heuristics select iteratively one or more quadrilaterals from the front, attach a new hexahedron to them, and update the front until the volume is completely meshed.

Calvo & Idelsohn [15] recently presented rough ideas of a recursive decomposition approach. They select a dual cycle to divide the combinatorial dual of the surface mesh into two subgraphs. This “cut” induces an interior two-manifold which is remeshed simply by mapping or projecting one of the obtained subgraphs onto it. However, fragments from previously used dual cycles are ignored in this mapping. This splitting process is applied recursively

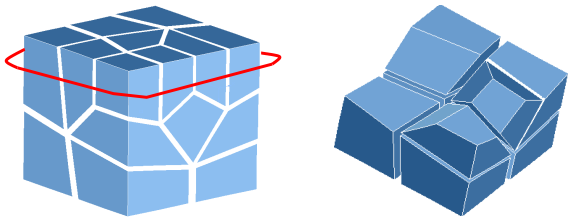

Figure 2: Example of a cycle elimination: The highlighted dual cycle is removed. This corresponds to the elimination of a complete sheet (layer) of hexahedra.

until there are no more unused dual cycles.

Whisker weaving [16, 17] first builds the combinatorial dual of a mesh and constructs the primal mesh and its embedding only afterwards.

1.3 Cycle Elimination Schemes

As mentioned above, the modified Whisker Weaving algorithm by Folwell & Mitchell [1], as well as a method proposed by the second author [2], rely on an iterative elimination of certain dual cycles in the surface mesh. More precisely, we regard the surface mesh as a planar graph and consider its graph-theoretical dual. Hence, for each primal edge of the surface mesh, there is a corresponding dual edge, and for each quadrilateral we have two pairs of edges lying opposite to each other. A cycle C in this dual graph is said to be a *canonical dual cycle* if for each edge $e \in C$ (corresponding to a primal edge of a quadrilateral in the surface mesh) the unique opposite edge is also contained in the dual cycle. See Fig. 2 for an example of a canonical dual cycle and the result after its elimination.

The crucial difference in these two approaches is that modified whisker weaving eliminates dual cycles without restrictions, whereas our approach requires canonical dual cycles with additional structural properties. Most importantly, all dual cycles should be free of self-intersections and a feasible elimination requires the mesh to be simple, planar and three-connected graph after each elimination. An ordering of all but the last three dual cycles with these properties is called a *perfect cycle elimination scheme*.

These restrictions on cycle eliminations, however, have one important advantage: Empirically, they are likely to yield meshes with a better structure. One possible measure to compare the internal connectivity structure of a combinatorial mesh is the distribution of node degrees. Clearly, large node degrees are to be avoided. The optimal node degree is that of a perfect grid, i.e. internal nodes should have six incident edges and eight hexahedra attached to it. For the mandible model, the maximal node degree of our hexahedral mesh is eight.

1.4 Overview and Contribution

The first major problem we have been faced with in the meshing process of the mandible model was the conversion of the given input triangulation into a coarse quadrilateral mesh. In Section 2 we describe the steps taken to generate such an initial quadrilateral mesh, called *macro element mesh* in the following. The surface of each macro element is represented as a *multi-patch* of the triangulation such that no information about the initial geometry is lost. The given very complicated free-form surface and its triangulation make a segmentation into nice clusters of triangles forming the multi-patches very difficult.

The key idea of our approach is to use an extremely coarse quadrilateral surface mesh which has a perfect cycle elimination scheme. A crucial property of a combinatorial, b-matching based mesh refinement algorithm described in [18] is the following: Given a surface mesh with a perfect cycle elimination scheme, any mesh refinement produced by our algorithm also has a perfect elimination order.

Then, in Section 3, we report recent advances in the cycle elimination approach. Experiments showed that a careful cycle selection is needed to reduce the size of the hex complexes and to improve their structure. We explain several new strategies which improve over previous methods:

1. a generalization of a cycle elimination to a multi-step cycle elimination;
2. a splitting into two submeshes by insertion of an internal 2-manifold;
3. a changed hex complex construction which allows to eliminate cycles which otherwise would imply an inferior mesh quality.

When we are dealing with mechanical parts there is often a “natural” decomposition into convex parts along clearly distinguishable sharp concave edges. In contrast, for the mandible model such a decomposition is not possible.

This has also consequences for the geometric embedding phase which we describe in Section 4. In the early stage of the development of our code we used the barycentric embedding algorithm (often referred to as *Laplacian smoothing*). However, for this simple to implement and fast algorithm it is well-known that it might fail to produce *valid* meshes (i.e., all elements are embedded inside

the domain and are non-inverted) for a non-convex domain. In addition, recent experiments with complicated whisker weaving meshes [19] show that this can also happen with convex domains. Therefore, following the pioneering work of Freitag and Knupp [20, 21, 19] we incorporated two additional embedding algorithms into our code. One algorithm is for local node position optimization based on the squared condition number of the Jacobian matrices attached to mesh nodes. The other algorithm is used "to untangle" the mesh, i.e., to find node positions such that all Jacobian determinants are strictly positive.

For the node position optimization of an untangled mesh, we apply a gradient based optimization routine with line search and thereby significantly increase the overall mesh quality. In contrast to reports by Freitag and Knupp [20] about numerical difficulties with this approach for tetrahedral meshes, our implementation seemed to work in a robust way for our test instances.

In Section 5, we apply the created hexahedral mesh to an interesting test case, and thereby show that we have achieved a mesh quality which allows a successful numerical analysis. In this experiment, we simulated a bite on a hard nut. The outcome agrees well with observations made in previous biomechanical experiments.

Finally, in Section 6, we summarize the main features of our approach and give directions for future work.

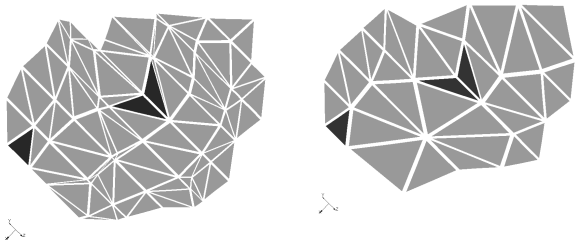

Figure 3: Removal of extreme triangles by iterated edge contractions.

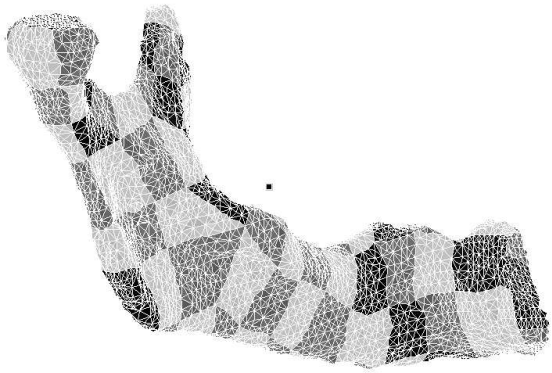

Figure 4: The clustering of one half of the mandible into multi-patches.

2 From Computed Tomography Data Towards a Quadrilateral Surface Mesh

The starting point of our investigation is a surface triangulation of the mandible with more than 35000 triangles. This data basis originally stems from computed tomography (CT) data from a tooth-less male. Iso-surfaces of the tissue density represented by the CT data are computed using the marching cubes method [22] with the help of SIPFaS[†].

The given initial triangulation contained numerous poorly shaped triangles (with minimum interior angle less than 5 degrees). To avoid numerical problems in the multi-patching and to reduce the size of the triangulation we applied iterative edge contractions as a first preprocessing step.

Fig. 3 shows the typical effect of this method for a small detail. Although this method reduces the mesh size already significantly, the triangulation is still too large by several orders of magnitude. Hence the next goal is a reduction to only about a few hundred multi-patches with the side constraint that the patches should be reasonably well-shaped.

2.1 Mesh Clustering and Multi-Patches

The simplification of surface triangulations (or more generally of polygonal surface meshes) has been intensively studied, mostly in computer graphics with the purpose of fast rendering, see the survey of Heckbert & Garland [23] for an overview.

Several methods have been developed which are specifically designed for the use in finite element meshes [24, 25, 26]. The most important clustering criteria in these approaches are region size, region curvature change (flatness), the preservation of sharp edges and corners, and simple boundary shape. These criteria are conflicting so that clustering methods usually take a weighted combination. However, the given triangulation is so "wild" (the "true" surface is smooth, whereas the triangulation preludes the existence of sharp edges) that it is not clear whether we can get satisfying results from these methods.

[†] SIPFaS (Simulated Interactive Plastic Facial Surgery) is a software package developed at TU Munich, chair of Applied Mathematics.

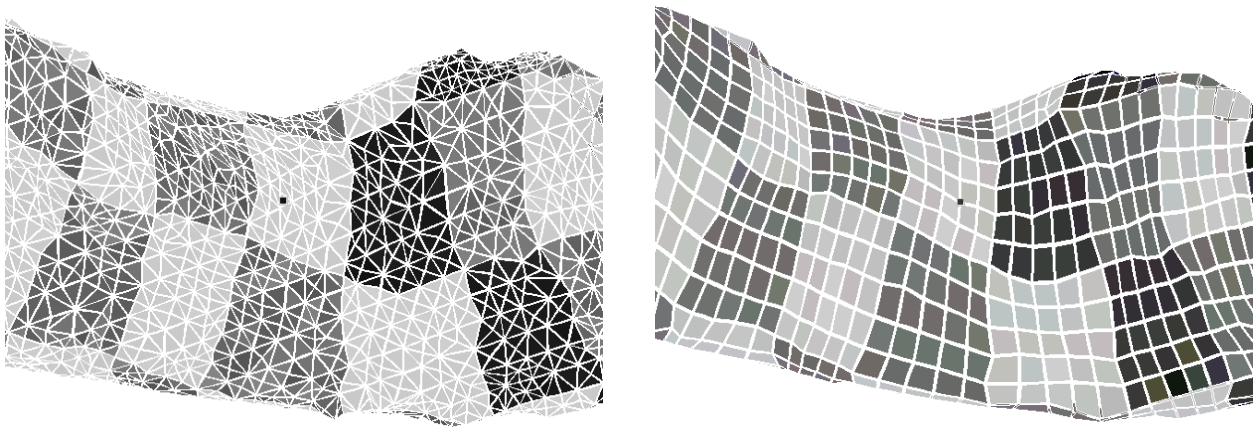

Figure 5: A detailed view on the multi-patches.

As long as this question is unsettled, we take a different approach, involving the following steps:

1. superimpose a very coarse but well structured quadrilateral surface mesh on the triangulation;
2. split all triangles which intersect with the boundary of quadrilaterals;
3. define clusters as all triangles lying inside a quadrilateral;

We partition the triangulation into clusters by coloring. This partitioning is induced by the equivalence relation that two triangles belong to the same cluster if they share an edge and are colored by the same color. Hence, uniformly colored sets of edge-connected triangles define a *cluster*.

See Figs. 4 and 5 for our clustering of the mandible model. The structure of the macro element mesh used for the clustering was designed by hand. For the embedding of this mesh onto the surface triangulation, the following procedure can be used: first, fix the position of certain macro element nodes on the surface. Given an appropriate coordinate system for the mandible model, one can choose extreme points with respect to the coordinate axes. Second, determine all other point positions by a variation of a stable projection technique [27].

2.2 Quadrilateral Mesh Refinement without Self-Intersecting Dual Cycles

With the clustering of the previous section we have achieved an extremely coarse quadrilateral mesh without self-intersecting dual cycles. The next step is to refine such a mesh to the desired mesh density keeping the property that all dual cycles are simple.

The recent paper [18] describes in detail how this can be achieved in a robust way: This method sets up and solves an auxiliary weighted b-matching problem defined on the dual of the surface mesh. The resulting b-matching solution is carefully decomposed into cycles and paths which can be realized and embedded as a quadrilateral mesh refinement without self-intersections.

Fig. 6 shows an example of such a refinement for the mandible model.

3 Improved Cycle Eliminations

As mentioned in the Introduction, the order in which cycles are selected for elimination has a great impact on the size of the resulting hexahedral mesh and of its quality. In this section, we describe two new strategies which are designed to reduce the size of the meshes.

3.1 Multi-Step Cycle Eliminations

We generalize the concept of a feasible elimination of a single dual cycle to a multi-step cycle elimination. (See [2, 28] for a detailed description of cycle eliminations.) A single cycle elimination on the surface graph corresponds in the construction phase to the addition of a sheet of hexahedra enclosed on one side of the cycle, the *elimination side* of a cycle.

A *k-step cycle elimination* selects k pairwise node-disjoint, simple cycles, say $C_1, C_2, \ldots, C_k$, for a simultaneous elimination and determines an elimination side

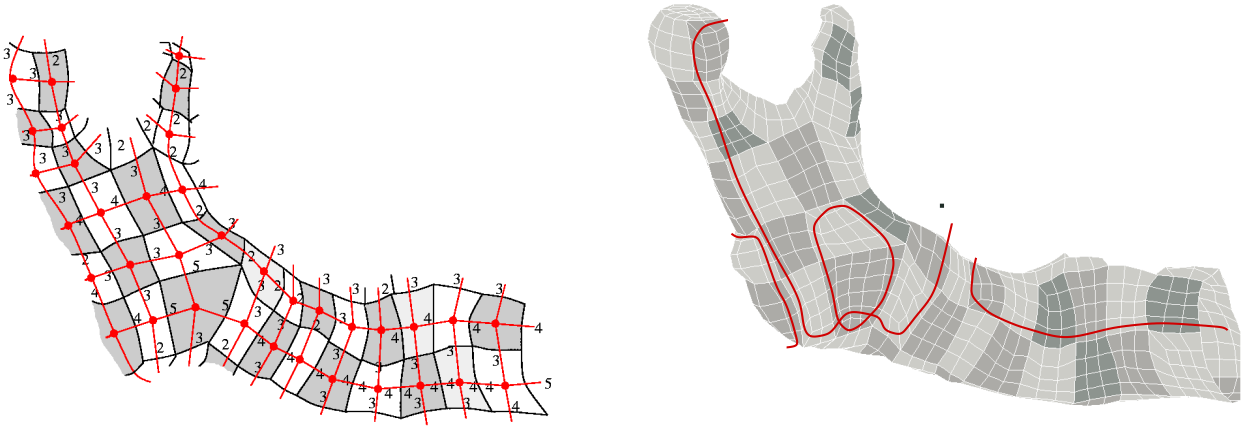

Figure 6: The b-matching problem defined on the dual graph of the coarse multi-patch quadrangulation, the given numbers attached to the edges are the b-matching values and denote the number of dual cycles crossing each primal edge (left), and the embedding without self-intersections of the b-matching decomposition into dual cycles (right).

for each of them. Denote by Q_i the enclosed quadrilaterals of cycle C_i on its elimination side, and let $Q = Q_1 \cap Q_2 \cap \cdots \cap Q_k$ be the common intersection. For a *feasible k-step cycle elimination* it is required that

1. the graph of the remaining cycle configuration is simple, planar and three-connected;
2. the set of quadrilaterals Q is edge-connected;
3. if $k > 1$, then the union $Q \cup Q_i$ contains more quadrilaterals than Q, for all $i = 1, \ldots, k$.

The hex complex is constructed sheet by sheet in reversed order of the cycle elimination in such a way that the new sheet is always placed onto the bounding surface of the so far constructed hex complex at the time it is added. More precisely, we place a new hexahedron on top of each quadrilateral contained in the set Q. Hence, we get a layer bounded by the selected cycles. In this sense, the new sheet is an *external sheet*. See Fig. 7 for an example where a 3-step elimination can be applied.

Note that an iterative elimination of the same set of cycles would lead to a larger hex complex (by the third condition on feasibility).

As for the special case $k = 1$ we can check feasibility of a k-step cycle elimination in linear time for any k.

3.2 Insertion of Internal Sheets

Suppose that a dual cycle C fulfills the structural criteria for a feasible elimination but the placement of an external sheet would lead to bad elements regardless which elimination side we would choose. Typically, this occurs in regions of local mesh refinements, see Fig. 8 for an example. For such cases, we now also allow the insertion of *internal sheets*. By that we mean a sheet which has only the quadrilaterals corresponding to the dual cycle in common with the current surface (so strictly speaking, the new sheet is only "almost internal"). Such a sheet is incident to all hexahedra lying directly below the enclosed quadrilaterals on the elimination side. See Fig. 9 for an example. For an internal sheet, we have the freedom to choose the smaller side with respect to the number of enclosed quadrilaterals as the elimination side. This typically leads to a remarkable reduction in the size of the hex complex.

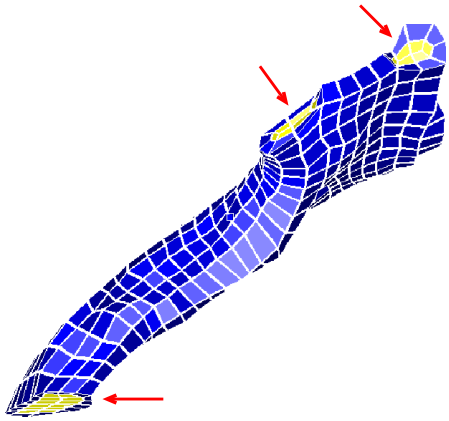

Figure 7: Example: Three-step-elimination (arrows point to the three selected dual cycles.

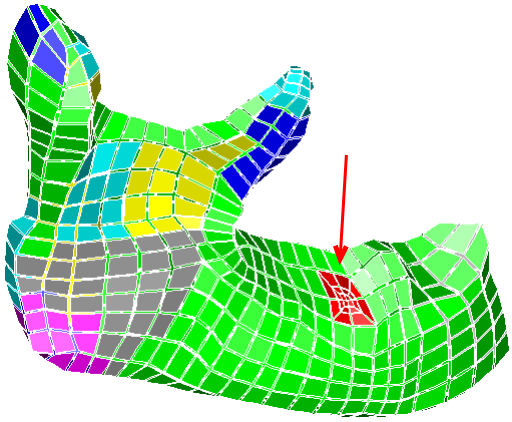

Figure 8: Local mesh refinement at the biting point (indicated by the arrow).

3.3 Decomposition into Subdomains

Practical experience shows that for achieving an acceptable mesh quality a dual cycle should only be eliminated and used in the construction as an external sheet if one of its neighboring primal cycles consists only of sharp edges. Hence, we are often faced with the problem that no dual cycle meets this elimination criterion. In such a situation a split into several subdomains is often very helpful. In contrast to Calvo & Idelsohn [15], we split the domain along a *primal* cycle of the current surface mesh and insert an additional internal two-manifold bounded by this primal cycle.

In [18], it has been explained how to find a suitable primal cycle for such a split and has been shown how to mesh such an internal two-manifold subject to the constraint that no self-intersection will be introduced in one of the two induced components.

We give an example for the mandible model where such a split has been performed. It yielded two almost equally sized submeshes, the left part of which is shown in Fig. 10. In this case, the internal surface consists of 28 quadrilaterals.

4 Mesh Optimization: Untangling and Smoothing

After the generation of a combinatorial hex complex, a careful geometric embedding is needed to get a valid mesh. By a *valid mesh* we mean that all elements are embedded inside the domain and are non-inverted. In the early stage of the development of our code we used only a barycentric embedding algorithm (Laplacian smoothing).

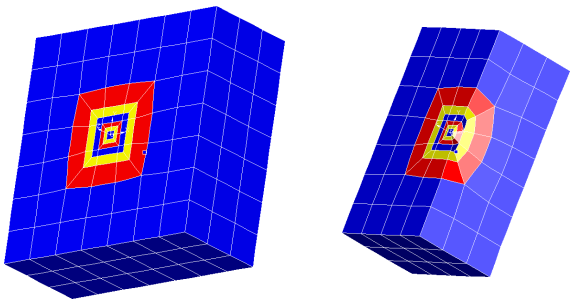

Figure 9: Example: Insertion of internal sheets.

However, for this simple to implement and comparably fast algorithm it is well-known that it might fail to produce valid meshes (and, indeed, it fails for our hexahedral mesh of the mandible).

Following the pioneering work of Freitag and Knupp [20, 19, 21] we incorporated two additional embedding algorithms into our code, one for mesh optimization and two for untangling.

4.1 Quality Measures

For a vertex of a hexahedron the Jacobian matrix is formed as follows. For that, let $x \in \mathbb{R}^3$ be the position of this vertex and $x_i \in \mathbb{R}^3$ for $i = 1, 2, 3$ be the position of its three neighbors in some fixed order. Using edge vectors $e_i = x_i - x$ with $i = 1, 2, 3$ the Jacobian matrix is then $A = [e_1, e_2, e_3]$. The determinant of the Jacobian matrix is usually called *Jacobian*. If the edge vectors are scaled to unit length, we get the *scaled Jacobian* with values in the range -1.0 to 1.0. An element is said to be *inverted* if one of its Jacobians is less or equal to zero. As the sign of a determinant depends on the order of its column entries, the latter definition is only useful for checking the quality of an element if the order of its neighbors is carefully chosen for each node. However, a consistent and fixed ordering of the nodes can easily be derived from the combinatorial hex complex by a graph search from some hexahedron lying at the bounding surface. Hence, in the following we will always assume that the numbering of the nodes is consistent for all hexahedra.

As a matrix norm, we always use the *Frobenius norm*, defined as $|A| = (tr(A^T A))^{1/2}$. The *condition number* $\kappa(A)$ of A is the quantity $\kappa(A) = |A||A^{-1}|$. For the evaluation of the mesh quality, we also use another hexahedral shape measure, the so-called Oddy metric [29], which can be written in matrix form as

$$f(A) = \det(A)^{-4/3}(|A^T A|^2 - \frac{1}{3}|A|^4).$$

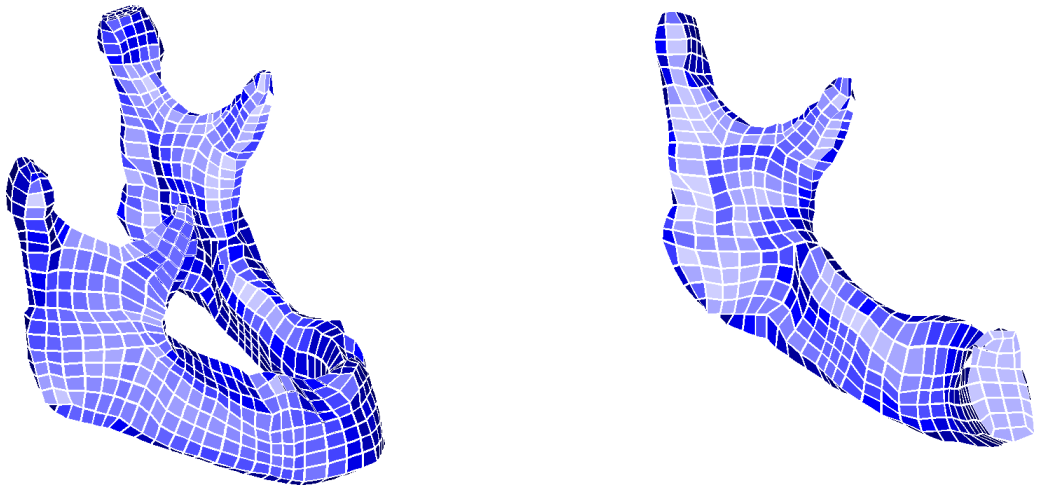

Figure 10: Hexahedral mesh for the mandible with 2252 elements (left), and one part of it after a split (right).

4.2 Optimization Based on the Condition Number

Let us assume for the moment that we have a valid mesh which we want to optimize with respect to the sum of the squared condition numbers as the objective function. This objective goes to infinity if some determinant approaches zero, but does not distinguish between inverted and non-inverted elements. Therefore, the modified condition number κ' is defined to be κ if the determinant is strictly positive and set to plus infinity, otherwise. In principle, one would like to minimize κ' over all hexahedra simultaneously; unfortunately, due to its size this global optimization problem is intractable.

This means that only iterative local node improvements based on this objective function restricted to the neighborhood of an interior node are possible, and this is the approach usually taken.

For the optimal node placement problem we compute a steepest descent direction and combine it with standard line search techniques to find an appropriate step size. (For details, see Dennis and Schnabel [30], for example.)

As a side constraint, we have to maintain the validity of the mesh. As a consequence, we need to check the Jacobians for all pairs of nodes and attached hexahedra incident to edges for which we want to change the position of one endpoint, which we call a *validity test*. Note that it does not suffice to check only the Jacobians attached to the node we want to move.

To implement these checks efficiently one has to provide an iterator data structure giving access to the elements to be checked in constant time per element. But even then, these checks seem to be too expensive if they are executed after each step. Therefore, we perform the validity test only after a constant number of steps and at the end of each node optimization phase. If we detect at such a point an invalidity, we backtrack to a valid stage. For that, we only need to store the node position at the beginning of a phase or immediately after the last successful check.

4.3 Mesh Untangling

The optimization procedure from the previous paragraphs requires a valid mesh as a starting point. Hence, we also implemented an algorithm which tries to maximize the minimum Jacobian of all the hexahedra attached to an interior node. To this end, we adapted in a straightforward way a local improvement procedure for tetrahedral meshes from Freitag and Knupp [20].

As mentioned above global optimization techniques are unlikely to work for very large meshes. However, in spite of our previous remarks we also experimented with a fairly general, global non-linear optimization technique for finite minimum-maximum problems. Namely, we used the Pshenichnyi-Pironneau-Polak algorithm [31]. This algorithm can be viewed as an extension of a gradient algorithm with an Armijo-type step-size rule. As a subroutine, it uses an enhanced version of the Frank-Wolfe algorithm to compute the search direction. We refer to the book of Polak [31] for details of this method. This algorithm is much more involved, may lead to efficiency problems for large meshes. However, for the moderate size of our meshes for the mandible model, it worked empirically very well.

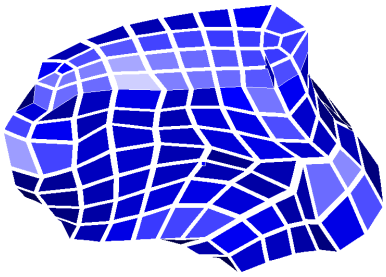

Figure 11: Part of the hexahedral mesh for the mandible.

4.4 Combined Embedding Algorithm

We use a combined embedding algorithm. To get a fast initial embedding, we use the barycentring smoothing algorithm. After the barycentring embedding a check is needed that all hexahedra are embedded inside the prescribed surface mesh. Nodes failing this check are moved into the domain. If the mesh is not valid after this initialization, we invoke an untangling phase. The number of iterations over all nodes is controlled by a termination criterion based on the maximum relative node movement within an iteration. Of course, this phase is also stopped immediately when the mesh becomes untangled. If the untangling phase terminates without finding a valid mesh, this may have two reasons: either we are stuck in a local minimum (if the local optimization procedure is used), or, if we are in a global minimum, the combinatorial mesh has no valid embedding. In any case, we start afterwards a gradient based optimization phase with respect to the squared condition number to improve the quality. If the mesh is still untangled, this is followed by a new invocation of the mesh untangling procedure.

4.5 Computational Results

Table 1 shows the results of the embedding phases with respect to different quality measures (scaled Jacobian, condition number, and Oddy metric) for the mandible mesh with 2252 hexahedra. For the interpretation, recall that the scaled Jacobian is to be maximized with an upper limit of 1.0, whereas condition number (with minimum 3.0), and the Oddy metric measure are to be minimized.

The initial barycentring embedding produces an invalid mesh with 39 inverted elements, and rather extreme values for the condition number and Oddy metric among the non-inverted elements. The first untangling phase considerably improves the mesh quality but still fails to yield a valid mesh as is contains one remaining inverted hexahedron. However, after a few optimization and untangling phases we get rid of all degeneracies and finally end up with a valid mesh and an overall average of 0.83 for the scaled Jacobian, 4.2 for the condition number, and 3.5 for the Oddy metric.

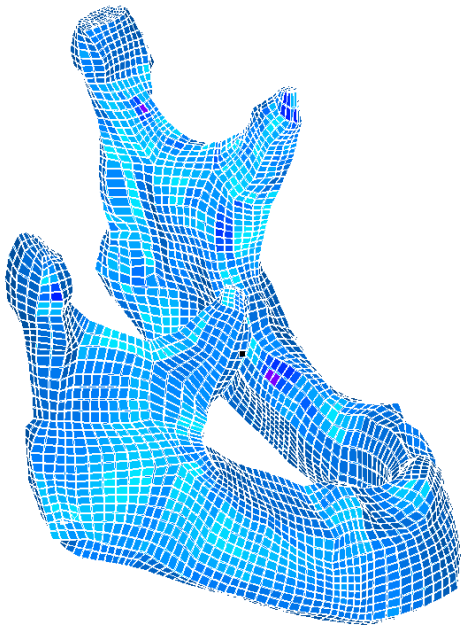

Figure 12: A refinement of the hexahedral mesh in Fig. 10 with 18674 hexahedra.

4.6 Ordering of the Hexahedra and Bandwidth

For the numerical linear algebra used in the FEM simulation the structure of the matrix assembled from the hexahedral mesh is of crucial importance. For example, it is desirable to find an ordering of the hexahedra which minimizes bandwidth or related parameters of the matrix. Due to its nature of our meshing algorithm to build up the mesh layer by layer, the created hex complex corresponds to an ordering of the hexahedra which is rather inefficient for the LR-decomposition.

Unfortunately, the bandwidth optimization problem and its variants are NP-hard. For the mandible, however, the simplest reordering strategy, namely a breadth first search, started from one boundary hexahedron at the left condyle, led to a decisive improvement.

quality measure	scaled Jacobian			condition number			Oddy metric			#inverted
	min	aver.	max	min	aver.	max	min	aver.	max	elements
barycentring embedding	0.001	0.817	0.999	3.01	4.46	1978.6	0.009	4.453	14355.4	39
after (first) untangling	0.048	0.813	0.999	3.01	4.37	95.1	0.009	3.677	779.4	1
final optimization	0.087	0.831	0.999	3.01	4.23	20.7	0.006	3.459	591.2	0

Table 1: Quality statistics for the embedding of the hexahedral mesh shown in Fig. 10 with 2252 elements.

5 Simulation: Bite on a Hard Nut

We now present the results of an FEM simulation with our coarsest hexahedral mesh. As an illustrative test case, we selected the situation of a lateral bite (on the right hand side). Based on the biomechanical experiments of Moog [32], the boundary loads were situated (the colors in Fig. 14 show the placement of the masticatory muscles and the biting point in our FEM model). For sake of a worst case test, a very "hard nut" is to be masticated. By that, we can assume approximately zero deformation at the biting point. In the mathematical modeling this is equivalent with the assumption of homogeneous Dirichlet boundary conditions. Bone tissue is modeled as homogeneous and isotropic, a linear material law is used with elasticity module of 11 GPa and Poisson number 0.28. A detailed discussion of the taken approach and its limitations goes beyond the scope of this paper. The interested reader is referred to Kober et al. [5].

For the FEM simulation we used the non-commercial FEM software package FeliCs [33][‡].

The ansatz described above allows the calculation of the biting force out of the FEM results. The orientation of the force vector (see Fig. 14) and the order of magnitude of its absolute value (here: about 600 N) give some hints on the quality of the simulations. Here, both lie in the realistic range. The same is true for the order of magnitude of the deformation ($5 \cdot 10^{-5} m$). Earlier studies have shown that von Mises equivalent stress is an appropriate post-processing variable [5]. Fig. 13 shows the von Mises equivalent stresses after the bite, with a maximum of about 9 MPa appearing directly at the area of the biting point. The deformation (100 times exaggerated) of the mandible is shown in Fig. 14. The shown results agree with observation from biomechanical experiments of Moog [32].

[‡] FeliCs has been developed at the chair of Applied Mathematics, TU Munich.

6 Summary and Future Work

We have presented a case study for the generation of hexahedral meshes with a high quality allowing successful FEM simulations in the field of biomechanics. As a first step, the given triangulation of a complex free-form geometry had to be converted into a suitable quadrilateral surface mesh. In absence of a robust clustering method, we took the approach to design a very coarse idealized macro element mesh for a mandible model by hand and to superimpose it on the given triangulation to form multi-patches. The creation of the idealized macro element mesh is done only once for the restricted domain of mandible models. This is an acceptable solution in view of the goal of an individual simulation with many variants of mandible models. But certainly more research on mesh coarsening applied to general free-from geometries for the purpose of quadrilateral meshing would be highly appreciated.

As soon as a coarse macro element mesh is available, we can use our mesh refinement techniques based on b-matching algorithms to yield a quadrilateral mesh refinement with any desired local mesh density (without self-intersecting dual cycles).

For the combinatorial phase of the hexahedral mesh generation, we presented new strategies for improved cycle elimination schemes. These methods effectively reduce the size of the hexahedral meshes and improve the structural quality of the meshes. In particular, we observed that most interior nodes have optimal degree six, and the maximal degree was only eight.

Gradient based mesh smoothing turned out to work well. At the current stage, we have concentrated our research concerning the embedding phase on finding the best quality, neglecting speed considerations to a certain degree. Future work must address the acceleration of the mesh embedding algorithms. Apart from further code fine-tuning we see potential for improved efficiency in the application of variants of quasi-Newton methods and other step-size rules in the line-search, as well as in more so-

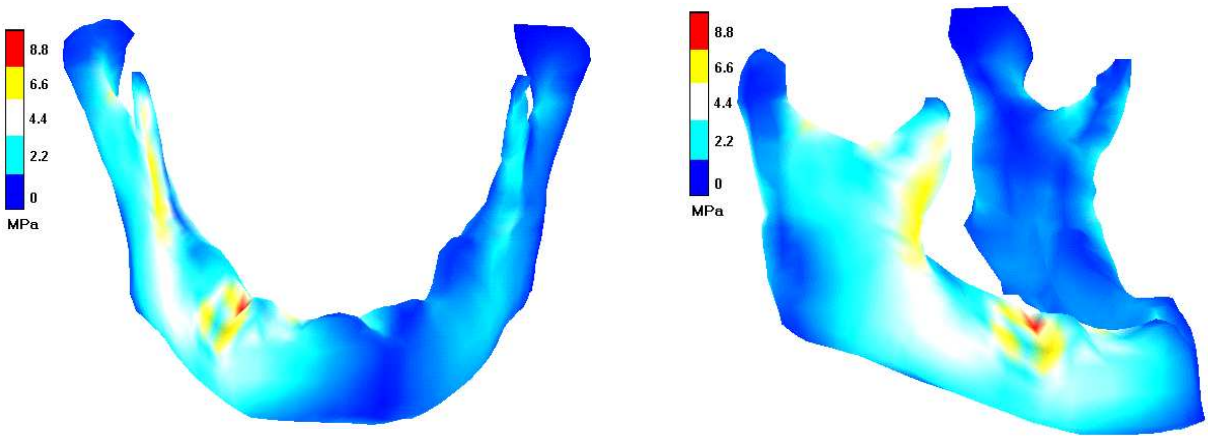

Figure 13: Von Mises equivalent stresses occurring at a lateral bite on a hard nut.

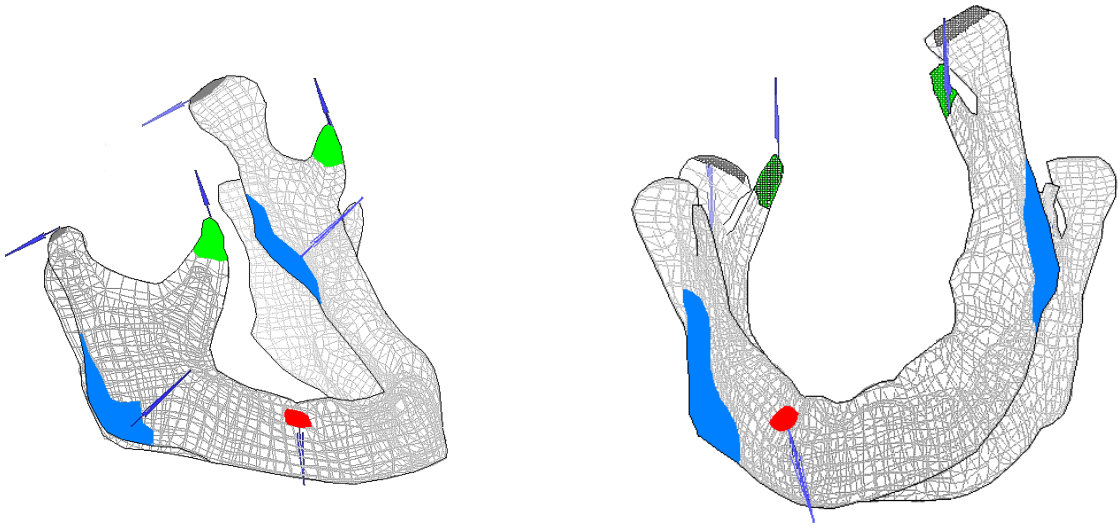

Figure 14: Deformation of the mandible (100 times exaggerated, order of magnitude $5.0 \cdot 10^{-5} m$) occurring at a lateral bite: the colors show the placement of the masticatory muscles and the biting point. The arrows indicate the assumed muscle forces.

phisticated node selection schemes for the order of local node optimizations.

We have presented one illustrative test case for the application of our hexahedral meshes to an FEM simulation of the human mandible. As noted above, our simulation results are in line with previous experiments. We have also successfully applied our mesh generation methods to a mandible model with a slightly different shape. Our current goal is to extend the simulation experiment and to study the effect of such a geometry change (a "sane" vs. an "ill" mandible) on the stress distribution and deformation after a bite.

Acknowledgments

The second author was partially supported by grants Mo 446/2-3 and Mo 446/2-4 of the Deutsche Forschungsgemeinschaft (DFG). He also wants to thank his students Benjamin Feldhahn, Steffen Hippler, Mathias Schacht, and Christian Trinks who worked hard on the implementation of his mesh generation algorithms.

The simulation of the mandible was made possible by a cooperation with H.-F. Zeilhofer and R. Sader from the Department of Oral and Maxillofacial Surgery at the University of Technology Munich.

Finally, the authors wish to thank G. Krause for providing us with the finite element preprocessor ISAGEN (which we used for our illustrations).

References

[1] Folwell, N. T., Mitchell, S. A. (1999) Reliable whisker weaving via curve contraction. *Engineering with Computers*, 15, 292–302.

[2] Müller-Hannemann, M. (1999) Hexahedral mesh generation by successive dual cycle elimination. *Engineering with Computers*, 15, 269–279.

[3] Kober, C., Sader, R., Thiele, H., Bauer, H.-J., Zeilhofer, H.-F., Hoffmann, K.-H., Horch, H.-H. (1999) Stress analysis of the human mandible related to traumatologic standard situations by numerical simulation (FEM) (in German). *To appear in Mund-, Kiefer- und Gesichtschirugie*.

[4] Kober, C., Sader, R., Thiele, H., Bauer, H.-J., Zeilhofer, H.-F., Hoffmann, K.-H., Horch, H.-H. (2000) Numerical simulation (FEM) of the human mandible: validation of the activity of the masticatory muscles (in German). *Biomedizinische Technik*.

[5] Kober, C., Bauer, H.-J., Zeilhofer, H.-F., Hoffmann, K.-H., Sader, R., Thiele, H., Deppe, H., Kliegis, U. (2000) FEM simulation of the human mandible: a preliminary step for new osteosynthesis techniques. In Stallforth, H. (editor), *Proceedings of Euromat99 — "Materials for Medical Engineering"*, Wiley-VCH.

[6] Schneiders, R. (1999) Quadrilateral and hexahedral element meshes. In Thompson, J. F., Soni, B. K., Weatherill, N. P. (editors), *Chapter 21, Handbook of Grid Generation*, CRC Press.

[7] Owen, S. (1998) A survey of unstructured mesh generation technology. http://www.andrew.cmu.edu/user/sowen/survey/ .

[8] Schneiders, R. Information on finite element mesh generation, http://www-users.informatik.rwth-aachen.de/~roberts/meshgeneration.html.

[9] Owen, S. Meshing research corner. http://www.andrew.cmu.edu/user/sowen/mesh.html.

[10] Thurston, W. (1993) Hexahedral decomposition of polyhedra. Posting to sci.math., 25 Oct., http://www.ics.uci.edu/~eppstein/gina/Thurston-hexahedra.html.

[11] Mitchell, S. A. (1996) A characterization of the quadrilateral meshes of a surface which admit a compatible hexahedral mesh of the enclosed volume. In *Proceedings of the 13th Annual Symposium on Theoretical Aspects of Computer Science (STACS'96)*. Lecture Notes in Computer Science 1046, Springer, 465–476.

[12] Eppstein, D. (1996) Linear complexity hexahedral mesh generation. In *Proceedings of the 12th Annual ACM Symposium on Computational Geometry, Philadelphia*, ACM, 58–67.

[13] Canann., S. A. (1992) Plastering: A new approach to automated, 3d hexahedral mesh generation. *Am. Inst. Aeronautics and Astronautics*, Reston, VA.

[14] Blacker, T. D., Meyers, R. J. (1993) Seams and wedges in plastering: A 3D hexahedral mesh generation algorithm. *Engineering with Computers*, 9, 83–93.

[15] Calvo, N. A., Idelsohn, S. R. (1998) All-hexahedral element meshing by generating the dual mesh. In

Idelsohn, S., Oñate, E., Dvorkin, E.(editors), *Computational Mechanics: New Trends and Applications*. CIMNE, Barcelona, Spain.

[16] Tautges, T. J., Blacker, T., Mitchell, S. A. (1996) The whisker weaving algorithm: A connectivity-based method for constructing all-hexahedral finite element meshes. *Int. J. Numer. Methods in Eng.*, 39, 3327–3349.

[17] Tautges, T. J., Mitchell, S. A. (1995) Whisker weaving: Invalid connectivity resolution and primal construction algorithm. In *Proceedings of the 4th International Meshing Roundtable*, Sandia National Laboratories, Albuquerque, 115–127.

[18] Müller-Hannemann, M. (2000) Improving the surface cycle structure for hexahedral mesh generation. In *Proceedings of the 16th Annual ACM Symposium on Computational Geometry, Hong Kong*, ACM, 19–28.

[19] Knupp, P. M. (2000) Achieving finite element mesh quality via optimization of the jacobian matrix norm and associated quantities, part II — a framework for volume mesh optimization. *Int. J. Numer. Methods in Eng.*, 48, 1165–1185

[20] Freitag, L. A., Knupp, P. M. (1999) Tetrahedral element shape optimization via the jacobian determinant and condition number. In *Proceedings of the 8th International Meshing Roundtable, South Lake Tahoe, CA*, Sandia National Laboratories, Albuquerque, 247–258.

[21] Knupp, P. M. (1999) Matrix norms & the condition number: A general framework to improve mesh quality via node-movement. In *Proceedings of the 8th International Meshing Roundtable, South Lake Tahoe, CA*, Sandia National Laboratories, Albuquerque, 13–22.

[22] Lorensen, W E., Cline, H. E. (1987) Marching cubes: High resolution 3d surface construction algorithm. *Computer Graphics*, 21, 163–169.

[23] Heckbert, P. S., Garland, M. (1997) Survey of polygonal surface simplification algorithms. In *Multiresolution Surface Modeling Course, SIGGRAPH'97*.

[24] Volpin, O., Sheffer, A., Bercevoir, M., Joskowicz, L. (1998) Mesh simplification with smooth surface reconstruction. *Computer-Aided Design*, 30, 875–882.

[25] Sheffer, A. (2000) Model simplification for meshing using face clustering. *To appear in Computer-Aided Design*.

[26] Inoue, K., Itoh, T., Yamada, A., Furuhata, T., Shimada, K. (1999) Clustering large number of faces for 2-dimensional mesh generation. In *Proceedings of the 8th International Meshing Roundtable, South Lake Tahoe, CA*, Sandia National Laboratories, Albuquerque, 281–292.

[27] Kobbelt, L. P., Vorsatz, J., Labsik, U., Seidel, H.-P. (1999) A shrink mapping approach to remeshing polygonal surfaces. In *EUROGRAPHICS'99 issue of Computer Graphics Forum*, 18, C119–C130.

[28] Müller-Hannemann, M. (1999) Shelling hexahedral complexes for mesh generation. Technical report no. 632/1999, Fachbereich Mathematik, Technische Universität Berlin.

[29] Oddy, A., Goldak, J., McDill, M., Bibby, M. (1988) A distortion metric for isoparametric finite elements. *Trans. CSME, No. 38-CSME-32, Accession No. 2161*.

[30] Dennis, J. E., Schnabel, R. B. (1983) *Numerical Methods for Unconstrained Optimization and Nonlinear Equations*. Prentice-Hall, Inc., Englewood Cliffs, NJ.

[31] Polak, E. (1997) *Optimization — Algorithms and Consistent Approximations*. Applied Mathematical Sciences, vol. 124, Springer.

[32] Moog, T. (1991) *Spannungsoptische Untersuchungen an unverletzten und frakturierten Unterkiefern*. PhD thesis, Universität Würzburg.

[33] Eichenseher, I., Götz, I. G. (1997) FeliCs — internal documentation. Technical report, Chair of Applied Mathematics, University of Technology Munich.